THE JOURNAL OF PHYSICAL CHEMISTRY A

Article

Cite This: J. Phys. Chem. A 2019, 123, 5928−5936

pubs.acs.org/JPCA

Ultrafast Solvation Dynamics Reveal that Octa Acid Capsule's Interior Dryness Depends on the Guest

Aritra Das,[†] Gaurav Sharma,[‡] Nareshbabu Kamatham,[‡] Rajeev Prabhakar,*[,‡] Pratik Sen,*[,†] and Vaidhyanathan Ramamurthy*[,‡]

[†]Department of Chemistry, Indian Institute of Technology Kanpur, Kanpur 208016, India

[‡]Department of Chemistry, University of Miami, Coral Gables, Florida 33146, United States

Supporting Information

ABSTRACT: Coumarins are well-known to exhibit environment-dependent excited-state behavior. We have exploited this feature to probe the accessibility of solvent water molecules to coumarins (guest) encapsulated within an organic capsule (host). Two sets of coumarins, one small that fits well within the capsule and the other larger that fits within an enlarged capsule, are used as guests. In our study, the two sets of coumarins serve different purposes: one is employed to explore electron transfer across the capsule and the other to release photoprotected acids into the aqueous environment. The capsule is made up of two molecules of octa acid (OA) and is soluble in an aqueous medium under slightly basic conditions. Molecular modeling studies revealed that while the OA capsule is fully closed with no access to water in the case of smaller coumarins, with the larger molecules, the capsule is not tight and the guest is in contact with water molecules, the number being dependent on the size of the coumarin. We have used the ultrafast time-dependent Stokes shift method to understand the solvent dynamics around the above guest molecules encapsulated within an OA capsule in an aqueous medium. Results depict that for the smaller sets of coumarins, water cannot access the guests within the OA cavity during their excited state lifetime. However, the case is completely different for the larger coumaryl esters. Distorted capsule structure exposes the guest to water, and a dynamics Stokes shift is observed. The average solvation time decreases with the increasing size of guests that clearly indicates accessibility of the encapsulated guests toward greater number of water molecules as the capsule structure distorts with increasing size of the guests. Results of the ultrafast solvation dynamics are consistent with that of molecular dynamics simulation.

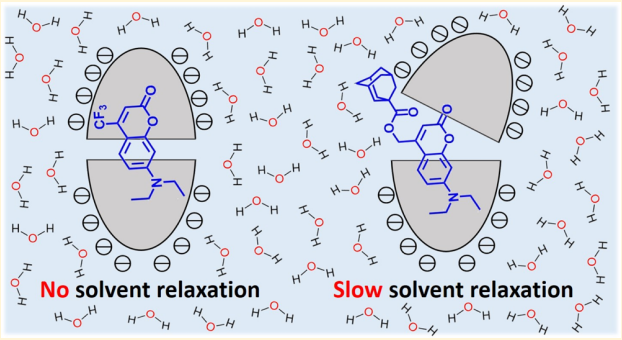

INTRODUCTION

During the last three decades, interest in understanding the physicochemical behavior and dynamics of molecules in confined spaces has grown steadily.[1−4] In this context, various organic and inorganic well-defined hosts have been employed as reaction space.[5−8] Our long-standing interest in exploring the photochemical and photophysical behavior of molecules in confined spaces[9,10] led us to use a synthetic molecule, octa acid (OA, Scheme 1), as the reaction medium.[11−13] In the presence of a guest molecule, two molecules of OA are assembled to form a capsule with the host to guest ratio of 2:1 or 2:2 in aqueous solution under basic conditions.[14] A variety of fluorescent as well as electron paramagnetic resonance active nitroxide probes revealed the interior of the capsule to be nonpolar and the micropolarity to be similar to that of benzene.[15,16] Considering that the capsule is present in an aqueous medium, absence of water molecules within the capsule was unanticipated. Fluorescence probes revealed that during the measurement time, the capsule neither disassembled nor partially opened to expose the probe molecules to the aqueous exterior. On the other hand, phosphorescence quenching of a variety of encapsulated guest molecules by oxygen indicated that the capsule partially opened and closed in the time scale of 5 μs.[17] The disassembling−assembling of the OA capsule takes place in the time-scale of 2.7 s that is 5 orders of magnitude slower than the partial opening and closing.[18] Thus, although in a nanosecond timescale, the capsule is intact, in a microsecond timescale, it partially opens and closes, and in a second time scale, it disassembles and assembles. The above conclusion is based on probes that are presumed to form a tight 2:1 capsule. Given that well-known hosts such as micelles, cyclodextrins, cucurbiturils, calixarenes, and related organometallic cavitands are permeable to water molecules, absence of water within the OA capsule is unique and provides an opportunity to conduct photochemical and photophysical studies under "dry" conditions even in an aqueous medium.

Received: May 15, 2019
Revised: June 17, 2019
Published: June 19, 2019

DOI: 10.1021/acs.jpca.9b04626
J. Phys. Chem. A 2019, 123, 5928−5936

Scheme 1. Structures of Water-Soluble OA Cavitand, and Guest Molecules; 1 (Coumarin-152), 2 (Coumarin-153), 3 (Coumarin-152A), and Coumaryl Esters 4−6

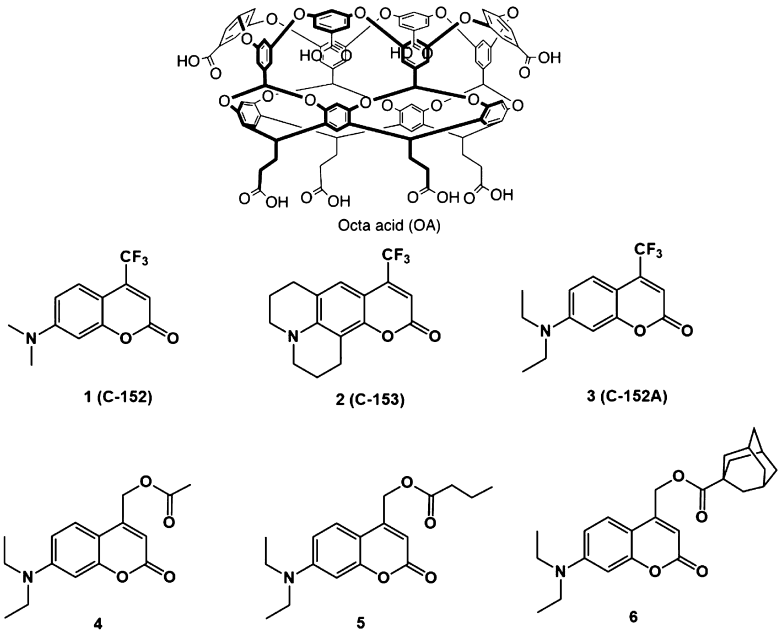

In a recent study, we established the occurrence of energy, electron, and spin communication between two molecules, one present within and the other outside the capsule.[19−27] The donors in this study were coumarin 152 (Scheme 1) and others of similar size and structure. Although we postulated that the above communications occurred through the capsular wall, until now, we do not have firm evidence to support the claim that the donor molecule remained within the capsule unexposed to the outside during its excited state lifetime. In contrast to this, using coumarin-based phototriggers of the type **4−6**, we succeeded in releasing an intermediate resulting from the excited state of the encapsulated guest.[28−32] This suggested that within the time period of the excited state of the phototrigger, the capsule at least slightly opened to let an intermediate come out (Scheme 2). These contrasting observations with smaller (**1−3**) and larger coumarins (**4−6**) prompted us to probe the ultrafast solvation dynamics[33−37] of OA-encapsulated coumarin probes of different sizes to ascertain water accessibility to the interior of the capsule. The expectation was that if the capsule remains completely closed during the excited state lifetime, there would not be any time-dependent solvation of the encapsulated guest by water molecules. On the other hand, if the capsule remains partially open during the excited state lifetime, the encapsulated guest would be solvated by water molecules and this could be monitored by ultrafast solvation dynamics experiments.

Coumarins such as **1−3** are known to show solvent polarity-dependent emission maxima, emission quantum yields, and S_1 lifetimes.[38] For example, excited **1** in cyclohexane emits fluorescence with a maximum of 395 nm and quantum yield of 0.49. On the other hand, in water, these are 456 nm and 0.055. This trend continues with a number of 7-amino-substituted coumarins.[38] This vast difference in emission characteristics between polar and nonpolar solvents has been exploited to monitor the solvent structure and its dynamics around coumarin molecules present in a variety of environments.[39−49] As mentioned above, based on several photophysical probes,

Scheme 2. Photocleavage of Coumaryl Esters 4−6 Leading to the Release of Acid (RCOOH) from the OA Capsule

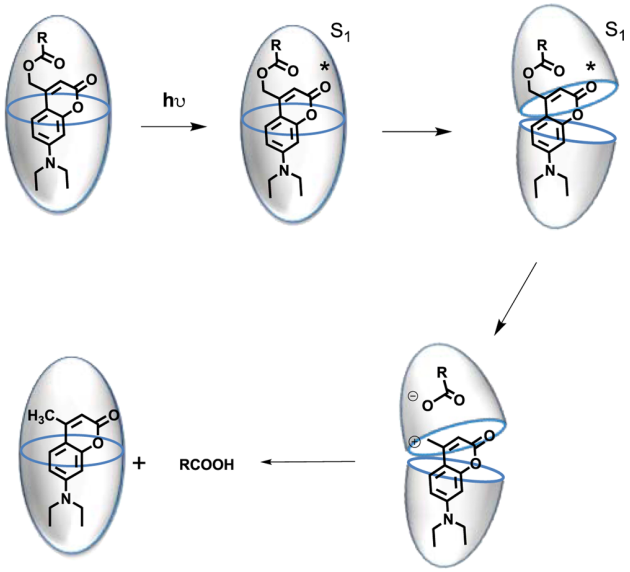

we have concluded that the interior of the OA capsule is dry and there are no water molecules. This suggested that the excited state guest molecules remain firmly locked within the capsule with no access to water molecules. However, with the change in the dipole moment of coumarins upon excitation, their exit from the capsule is a likely possibility. We believed that if the ground-state coumarin is present in a "dry" capsule, the photophysical characteristics would be similar to that of benzene. Upon excitation, if the capsule does not open and the guest stays within, the surroundings of the excited coumarin would be similar to that of the ground-state one. Under such conditions, there would be no change in emission characteristics if there are no water molecules near the excited probe.

DOI: 10.1021/acs.jpca.9b04626
J. Phys. Chem. A 2019, 123, 5928−5936

This is expected to be the case when the capsule is compact. On the other hand, if the capsule structure is distorted, exposing the guest molecule to the surrounding water, the photophysical characteristics would change from that in benzene to that in water. With this expectation in mind, we performed ultrafast solvation dynamics experiments with the coumarins **1**−**3** listed in Scheme 1. As mentioned above, the photobehavior of OA-encapsulated **4**−**6** is different from that of **1**−**3**. This suggested that solvation dynamics around these is likely to be different from that around **1**−**3** in OA. This prompted us to pursue ultrafast solvation dynamics studies of OA-encapsulated **4**−**6**. An insight into the structure of OA complexes of **1**−**6** obtained through molecular modeling, including docking and molecular dynamics (MD) simulations, was exceptionally useful in understanding the different solvation dynamics obtained with the two groups of coumarins, smaller **1**−**3** and larger **4**−**6**. According to molecular modeling, guests **1**−**3** are present in a dry capsule, whereas **4**−**6** are present in a slightly distorted capsule in touch with one or more water molecules.

The complimentary experimental and theoretical approaches employed here have provided a unique understanding of the dynamics of OA-encapsulated excited coumarins, **1**−**6**, in ultrafast time domain. Results discussed here suggest that the OA capsules with smaller coumarins, **1**−**3**, as guests that are used as donors in electron-transfer experiments remain tight within the capsule during their lifetime and the ones with larger coumarins, **4**−**6**, as guests, which are used as phototriggers, keep the guests exposed to increasing number of water molecules during their lifetime.

EXPERIMENTAL SECTION

Materials. Coumarins C-152, C153, and C152A were used as received from Sigma-Aldrich/Alfa Aesar. Coumarins **4**, **5**, and **6** were synthesized by following a reported procedure.[31] The host, OA, was synthesized by following the literature procedure.[13]

Instruments. UV−vis spectra were recorded on a commercial spectrophotometer (UV-2600 or UV-2450, Shimadzu, Japan); emission spectra were recorded on a commercial fluorimeter (FS920CDT, Edinburgh, UK or FluoroMax-4, Jobin Yvon, USA).

For fluorescence lifetime measurements in picosecond resolution, a commercial time correlated single photon counting (TCSPC) setup (LifeSpec II, Edinburgh Instruments, UK) was used. The instrument uses a thermoelectrically cooled Hamamatsu R3809-50 MCP PMT as the detector. A 375 nm diode laser (EPL-series, Edinburgh Instruments) with 80 ps pulse width was used as the excitation source. The instrument response function (IRF) was found to be 120 ps. The fluorescence transients were fitted triexponentially following deconvolution with the IRF.

Femtosecond fluorescence upconversion experiments were performed in a commercial setup (FOG-100, CDP Corp., Russia). In brief, the 800 nm output of a mode-locked Ti:sapphire laser (Mai Tai HP, Spectra Physics, USA) was used to generate 400 nm light on a 0.2 mm β-barium borate (BBO) crystal. This second harmonic light is then used to excite the sample taken in a rotating sample cell under the magic angle condition. The pump power is maintained to be 4 mW. The fluorescence emitted from the sample is then mixed with the fundamental light 800 nm on a 0.5 mm BBO crystal to generate the sum frequency light that was then dispersed by a monochromator and detected with a photomultiplier tube. One feet mechanical delay stage was used to control the arrival time of the gate pulse on the BBO crystal and in that process, we scan the emitted fluorescence in a 2 ns time window. The IRF was found to be Gaussian in nature having full width at half maxima of 250 fs. The recorded fluorescence transients were deconvoluted using the measured IRF with the help of the commercial software, Igor Pro.

Sample Preparation of Host−Guest Complexes for ^{1}H NMR Experiments. A solution of 600 μL of 1 mM OA (in 10 mM $Na_2B_4O_7$ in D_2O, pH = 8.7) was placed in an NMR tube. Then, 0.25 equiv increments of the guest solution (2.5 μL of a 60 mM solution in DMSO-D_6) were added. After shaking the NMR tube for 5 min, the ^{1}H NMR spectrum was recorded to confirm the complex formation. The complex formation was monitored by the upfield shift of the aliphatic proton peaks of the guest.

Sample Preparation of Host−Guest Complexes for Absorption and Steady State and Time Resolved Fluorescence Experiments. A 60 mM stock solution of the guest in DMSO-D_6 and 60 mM stock solution of the host OA in phosphate buffer/H_2O were prepared. Solutions of varying stoichiometric ratios of the host and guest were prepared by titrating increasing amounts of the OA stock solution into 4 mL of phosphate buffer solution containing 2.5×10^{-5} M guest. Absorption and emission spectra were recorded for the same solution. Addition was stopped when there was no further change in the emission spectrum. The same stock solutions were used for time-resolved experiments. A buffer solution containing 10×10^{-5} M guest and 5 equiv of host was used for these experiments. Complexation was confirmed by steady-state spectra before performing the time-resolved studies.

Molecular Modeling Procedure. The structure of OA was taken from our previous work,[50] and the guest molecules were modeled using the GaussView program. The Gaussian 09 program[51] was used to optimize OA and guest molecules without any geometrical constraint at the B3LYP[52]/6-31g(d)[53] level. Molecular docking was performed to investigate the binding of the guest molecule to the OA using the AutoDock Vina 1.5.6 program.[54] The size of the grid was chosen to cover the entire cavity of OA, and the spacing was kept to 1.00 Å, which is a standard value for AutoDock Vina. The docking procedure yielded 20 poses, and the structures with the highest scoring function were used for the MD simulations. The GROMACS 4.5.6 program[55] utilizing the AMBER 03 force field[56] was used to perform these simulations of the OA−guest complexes. Antechamber, an inbuilt tool in AMBER, was used to calculate the restrained electrostatic potential charges and making topology files.[57] The starting structures were placed in a cubic box with dimensions of $60 \times 60 \times 60$ Å and was then filled with TIP3P water molecules.[58] To neutralize the system, some of the water molecules were replaced by Na^+ ions and the system was energy minimized for 3000 steps. They were used to study the OA−guest interactions through all-atom 100 ns MD simulations. The MD simulations were carried out with a constant number of particles (N), pressure (P), and temperature (T) (NPT ensemble). Electrostatic interactions were calculated using the particle mesh Ewald method,[59] and a cutoff at 1.2 nm was used for both van der Waals and Coulombic interactions. The bond lengths and angles of the water molecules were constrained by the SETTLE[60] algorithm, and the LINCS[61] algorithm was used to constrain the bond

DOI: 10.1021/acs.jpca.9b04626
J. Phys. Chem. A 2019, 123, 5928−5936

lengths of the OA. The MD trajectories were computed for each model with a time step of 2 fs. Cluster analysis was performed to derive the most representative structures of the OA−guest complex. YASARA,[62] Chimera,[63] and VMD[64] programs were used for the visualization and preparation of the structural diagrams presented in the current study.

RESULTS

According to ^{1}H NMR study, six guests listed in Scheme 1 formed 2:1 host−guest complexes with OA in a phosphate or borate buffer. Hydrophobic feebly water-soluble **1**−**6** formed transparent solutions in the presence of OA at pH ∼8.9 (borate buffer). Observed upfield shift of N-alkyl group confirmed the inclusion of the above guests within OA (Figure S1).[13−15] As a representative, ^{1}H NMR spectra of **4** in the presence of OA are shown in Figure 1. Lack of changes in the

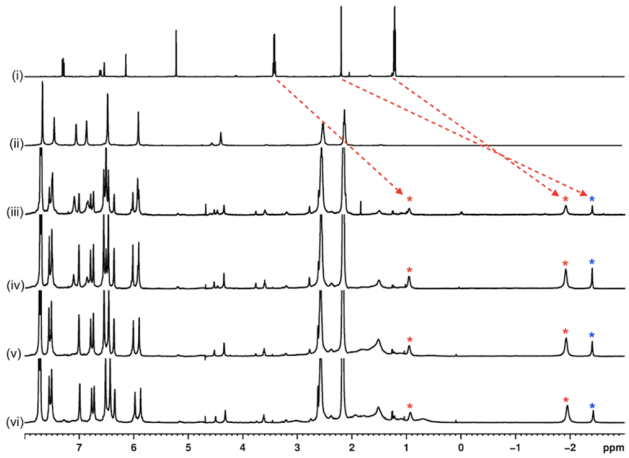

Figure 1. ^{1}H NMR (500 MHz, 10 mM $Na_2B_4O_7$ buffer/D_2O, pH = 8.7) spectra of (i) **4** in $CDCl_3$; (ii) **1**@OA ([OA] = 1 mM and [**1**] = 0.25 mM); (iii) **4**@OA ([OA] = 1 mM and [**1**] = 0.5 mM); (iv) **4**@OA ([OA] = 1 mM and [**1**] = 0.75 mM); (v) **1**@(OA ([OA] = 1 mM and (vi) [**1**] = 1.0 mM); "blue *" and "red *" indicate the OA-bound guest proton peaks, red ■ indicates the residual solvent peak (water) of D_2O.

spectra when more than half equivalent of the guest was added to the host in the buffer suggested the ratio of the host to the guest in the capsule to be 2:1 (see Figures S2 and S3 for **5** and **6**). Furthermore, careful ^{1}H NMR titration experiments supported the above conclusion. Consistent with the capsule formation, the diffusion constants were measured to be closer to 1.35×10^{-6} cm^2 s^{-1} (Table S1 for **5** and **6**). It is known that the diffusion constants of free OA and 1:1 open cavitandplex are 1.88×10^{-6} and $\sim 1.7-1.9 \times 10^{-6}$ cm^2 s^{-1}, respectively.[14,15] The reduced diffusion constant noted above for **4**@OA_2 is a clear indication of the formation of a capsular assembly rather than an open 1:1 cavitandplex. Furthermore, as expected for a 2:1 capsule (two OA and one guest molecules), the integrations of the NMR peaks of the host (H_f) and the guest, *N*-dimethyl protons of the solution, containing no free host or guest were 8:6 (a capsule will have 8 H_f protons). Upon addition of the guest to the OA buffer solution, there were NMR signals only because of the complexed guest which remained constant, independent of the amount of the guest present in solution, and only the intensity changed. No signals due to a free guest were seen. This suggested that there was no exchange between the complexed and uncomplexed guest molecules. In the absence of exchange, we could not generate a Job plot to obtain the host−guest ratio. Finally, till now, OA−guest complexes could not be crystallized. This prevented unequivocal confirmation of the host−guest ratio.

Inclusion of guests within OA is also revealed by the changes in the emissions spectra upon gradual addition of OA to a buffer solution of **4** (Figure 2c). It is clear that the emission maximum of 506 nm in water steadily shifted to 451 nm upon addition of OA to the buffer solution of **4** (see Figure S4 for **5** and **6**). The latter value is closer to that in benzene (Figure 2b). A similar observation was also made from the absorption spectra (Figure 2a). Considering that the polarity of the capsular interior has been inferred to be similar to that of benzene, the observed shift confirmed that upon addition of OA, the guest **4** is included within the OA capsule. Similar shift in the absorption and emission observed for other coumarins used in this study (Figures S5) confirmed their inclusion within the OA capsule.

Structures of the OA-encapsulated guest molecules **1**−**6** in water obtained from molecular modeling are provided in Figures 3 and 4. The difference in the structures between the two sets of molecules, especially in terms of water penetration into the capsule must be noted. In the case of **1**−**3**, the coumarins are in a dry hydrophobic environment with nearest water molecules being hydrogen bonded to the carboxylates projecting away from the capsule. On the other hand, **4**−**6** are in a less hydrophobic environment and are bonded to at least one water molecule. In these cases, the capsule is slightly ajar in the middle, the extent being dependent on the bulkiness and

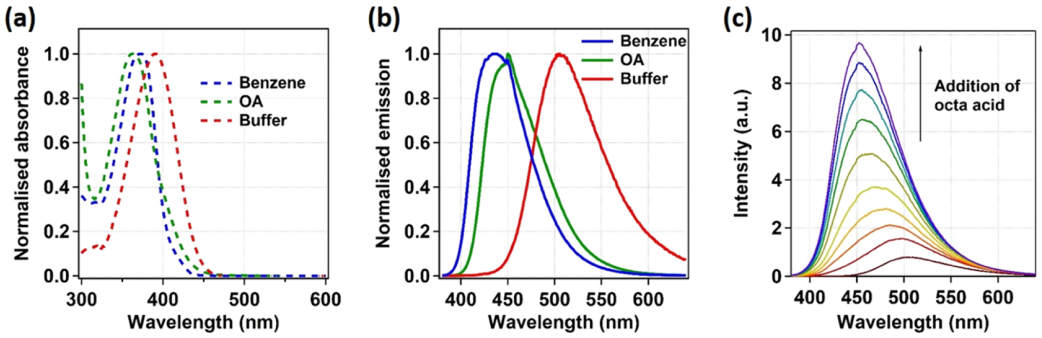

Figure 2. (a) Normalized absorption spectra, (b) normalized emission spectra of **4** in benzene (blue), **4**@$(OA)_2$ (green), and **4** in buffer (red); ([**4**] = 2.5×10^{-5} M, [OA] = 5×10^{-5} M in phosphate buffer/H_2O, pH = 7.4), and (c) fluorescence titration spectra (λ_{ex} = 370 nm) of **4** with addition of OA.

DOI: 10.1021/acs.jpca.9b04626
J. Phys. Chem. A 2019, 123, 5928−5936

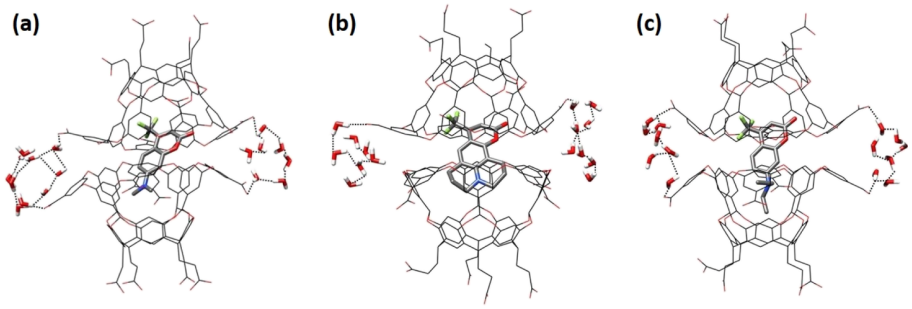

Figure 3. MD simulated structure for (a) **1**@OA_2, (b) **2**@OA_2, and (c) **3**@OA_2 in water.

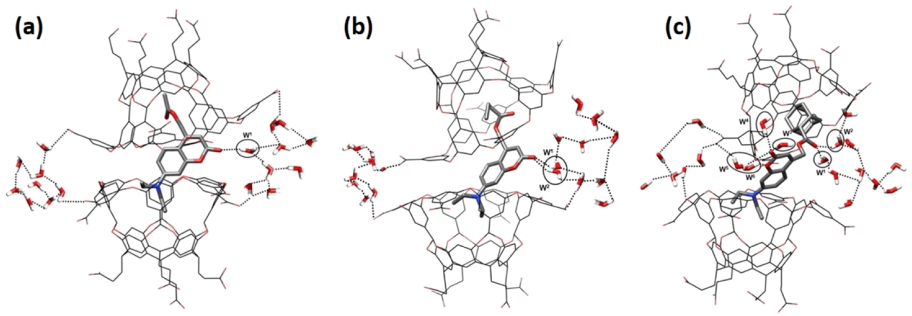

Figure 4. MD simulated structure for (a) **4**@OA_2, (b) **5**@OA_2, and (c) **6**@OA_2 in water.

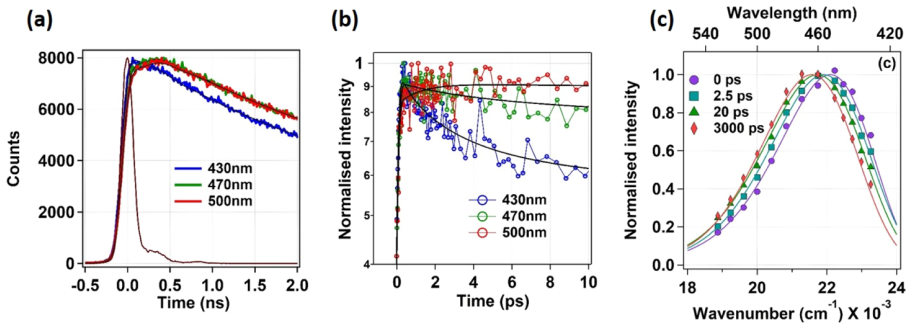

Figure 5. (a) Representative TCSPC decay profile at some selected wavelengths, (b) representative ultrafast fluorescence transients at some selected wavelengths, and (c) TRES constructed from the combination of femtosecond fluorescence upconversion and TCSPC method for **6**@OA_2

size of the guest. The trend is clear; **4** is hydrogen bonded to one molecule, **5** to two molecules, and **6** to at least six molecules of water.

Having confirmed by ^{1}H NMR that **1**−**6** formed 2:1 capsular assemblies with OA, we proceeded to perform ultrafast time-resolved experiments to probe the change of environment around the guest molecule. In this context, we have carried out both TCSPC and femtosecond fluorescence upconversion experiments to find the average solvation time for all six OA complexes. Results with **4**−**6** are presented first. We have presented the time-resolved emission spectra (TRES) and representative fluorescent transients measured by TCSPC and upconversion method at some selected wavelengths for **6**@OA_2 in Figure 5. The same for **4**@OA_2 and **5**@OA_2 are shown in Figure S6 of the Supporting Information. TCSPC measurements revealed substantial dynamic Stokes shift in case of **4**@OA_2. Because similar shift was not observed with **5**@OA_2 and **6**@OA_2 by TCSPC measurements, we undertook the femtosecond fluorescence upconversion study. TRES for all three cases were generated using the fitting parameters of the fluorescence transients. Combined results of upconversion and TCSPC identified the dynamic Stokes shift in these cases. Results of these are displayed in Figures 5c and S5c,f. The average solvation time for these three complexes was estimated from the solvent response function, $C(t)$. As shown in Figure 6, the plot of solvent response function with respect to time fitted

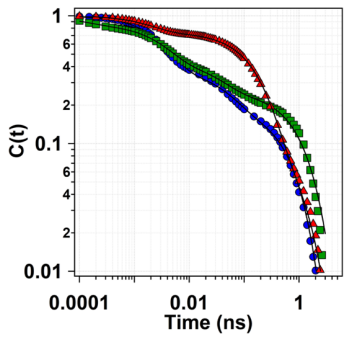

Figure 6. Variation of solvent response function with time for **4**@OA_2 (red triangle), **5**@OA_2 (green square), and **6**@OA_2 (blue circle).

DOI: 10.1021/acs.jpca.9b04626
J. Phys. Chem. A 2019, 123, 5928−5936

into a triexponential function. Table 1 lists various parameters for **1**–**6** extracted from absorption, emission, and ultrafast time-resolved experiments.

Table 1. Solvation Dynamics Parameters for 1–6 Encapsulated within OA Cavity

host–guest complex	λ^{abs}_{max} (nm)	λ^{em}_{max} (nm)	$\lambda^{em}_{0\ ps}$ (nm)	$\lambda^{em}_{3000\ ps}$ (nm)	observed shift (nm)	average solvation time (ps)
1@OA_2	384	446	446	446	nil	not applicable
2@OA_2	416	480	478	480	nil	not applicable
3@OA_2	385	453	454	453	nil	not applicable
4@OA_2	359	446	422	446	25	440
5@OA_2	379	450	437	449	12	250
6@OA_2	389	465	454	465	11	144

This led us to examine the solvation dynamics of **1**@OA_2, **2**@OA_2, and **3**@OA_2 that according to molecular modeling remain fully enclosed and away from water molecules. As anticipated, upconversion and TCSPC experiments did not reveal any change in emission spectra as a function of time. TRES and representative fluorescent transients measured by TCSPC and the upconversion method at some selected wavelengths for **3**@OA_2 are depicted in Figures 7, and S7 of the Supporting Information displays the same for **1**@OA_2 and **2**@OA_2. The lack of variation of the emission spectra with time is consistent with the conclusion that there are no changes in the environment around enclosed **1**–**3** during their excited state lifetime.

DISCUSSION

As mentioned in the Introduction section, coumarins **1**–**3** were used as donors in our studies on electron transfer across the capsular wall of OA.[19−21] To be able to accurately interpret the results, we needed to know whether there is any physical contact between the encapsulated donor and the acceptor present outside the capsule. This led us to obtain the structures of the OA complexes by MD simulation and ultrafast solvation dynamics. In this context, MD simulated structures presented in Figure 3 and the TCSPC decay profiles, ultrafast fluorescence profiles, and TRES displayed in Figure 7 are revealing. The structures for **1**–**3**@OA_2 generated by MD simulations in water share common features: the guest remains aligned vertically along the long axis of the capsule with the hydrophilic carbonyl group away from the median of the capsule. More importantly, there are no water molecules near the guest. The two halves of the capsule appear tightly closed pushing the water molecules to the periphery. This is the equilibrated ground-state structure from where light absorption occurs.

The most important question is whether there are changes following excitation, especially in terms of their immediate environment. Such changes could lead the excited guest to be in contact with the acceptor outside. Data presented in Figure 7 show that this is not the case. Particularly important spectra to note are the TRES shown in Figure 7. In none of the three molecules, during the initial 3000 ps time period, is there a shift in the spectra. The emission maxima for **1**, **2**, and **3** immediately upon excitation (0 ps) are 446, 478, and 454 nm. Even after 3000 ps, there is very little shift, 446, 480, and 453 nm, respectively (Table 1). Given that these coumarins are well known to display solvent polarity-dependent emission maxima, a lack of shift when confined in an OA capsule confirms that the environment around the three coumarins is the same during their excited state lifetime. Comparison of the behavior of **1**–**3** with **4**–**6** (discussed below) reinforces the conclusion that the coumarins **1**–**3** remain within the capsule and are not exposed to water or any other molecules all through their excited state lifetime.

As described in an earlier publication, molecules **4**–**6** upon excitation release acids (acetic acid, propionic acid, and adamantyl carboxylic acid, respectively) to the aqueous exterior.[28−32] As illustrated in Scheme 2, excitation of **4**–**6** leads to α-cleavage leading to two radical intermediates, leaving one inside and extruding the other to the aqueous exterior. Obviously, for this to happen unlike the capsules of **1**–**3**, that of **4**–**6** will have to open up at some stage after excitation. If this occurs during the excited state lifetime of **4**–**6**, the ultrafast solvation dynamics of these molecules must be different from that of **1**–**3**.

A comparison of Figures 3 and 4 reveal that the MD simulated structures of these two sets of complexes are different. The capsules containing **4**–**6** are slightly distorted and even have a few water molecules seeping into them. The extent of distortion and how many molecules of water interact with the guest depend on the size of the guest. The largest adamantyl-substituted one has at least six molecules of water in contact with the encapsulated guest. Because the parent chromophore in **4**–**6** is the same, the absorption and emission characteristics are expected to be the same, provided the environment surrounding them is identical. However, the absorption and emission maxima listed in Table 1 show that

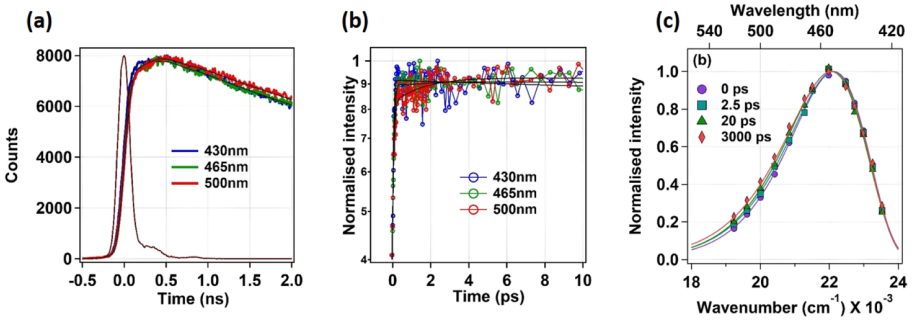

Figure 7. (a) Representative TCSPC decay profile at some selected wavelengths, (b) representative ultrafast fluorescence transients at some selected wavelengths, and (c) TRES constructed from the combination of femtosecond fluorescence upconversion and TCSPC method for **3**@OA_2.

DOI: 10.1021/acs.jpca.9b04626
J. Phys. Chem. A 2019, 123, 5928−5936

this is not the case. Clearly, the microenvironments around **4**–**6** are not identical, a conclusion consistent with the results of the MD simulations.

We have been able to capture most of the dynamic shift for encapsulated **4** with TCSPC, whereas for **5** and **6**, the TCSPC measurement did not show any significant dynamic Stokes shift. This implies that for **4**, the solvent relaxation process is much slower compared to that in the cases of **5** and **6**. To capture the dynamic Stokes shift in the case of OA-encapsulated **5** and **6**, we performed solvation dynamics study in the femtosecond fluorescence upconversion mode. The results obtained are shown in Figure 5. Important information about the dynamics is provided by the solvation time, which is slow for **4** (440 ps), medium for **5** (250 ps), and relatively fast for **6** (144 ps). The origin of the difference in solvation time, we believe, rests in the initial excited structure within OA that gets solvated and the number of nearby water molecules. We believe that solvation must start from vertically excited, vibrationally relaxed structures of **4**, **5**, and **6**. Such structures must in reality be closer to the MD simulated ground-state structures shown in Figure 4. The difference between the two groups of molecules (**1**–**3** and **4**–**6**) becomes obvious upon perusal of Figures 5 and 7 and upon noting the emission maxima at 0 and 3000 ps time. In the case of **1**–**3**, the emission maxima are identical at 0 and 3000 ps and the TRES do not change with time (Figure 7). However, in the case of **4**, **5**, and **6**, there is a significant shift between 0 and 3000 ps: 25, 12, and 11 nm, respectively. The TRES shown in Figure 5 clearly recorded the shift with time. The above shift suggests that the guest molecules' environment is changing with time.

CONCLUSIONS

In this study, we have focused on bringing out the difference between the two groups of coumarin-based guest molecules. Our interest in these systems arises from their use as electron donors and as phototriggers. We have demonstrated through ultrafast solvation dynamics studies that small coumarins such as **1**–**3** remain enclosed within the OA capsule with no contact with water molecules during their excited state lifetimes. The second set of coumarins, **4**–**6** have traditionally been used as phototriggers. Upon inclusion within the OA capsule, these molecules remain in touch with a few molecules of water and upon excitation, there is some dynamic within the capsule which probably facilitates the release of a fragment of the molecule (Scheme 2). A comparative ultrafast solvation dynamics investigation of the six molecules has brought out the extent of water inclusion and dynamics of the guest and nearby water molecules, depending on the size and structure of the guest molecules. Detailed understanding of the dynamics of water molecules near the capsule opening and the origin of slow solvation time is likely to provide a better understanding of water structure in confined spaces.

ASSOCIATED CONTENT

Supporting Information

The Supporting Information is available free of charge on the ACS Publications website at DOI: 10.1021/acs.jpca.9b04626.

Structures of the molecules used in this study, ^{1}H NMR spectra of host–guest complexes, ^{1}H NMR and fluorescence titration spectra of guests with OA, fluorescence and absorption spectra of guests and host–guest complexes, representative TCSPC and femtosecond fluorescence up-conversion traces, TRES, and diffusion constant of host–guest complexes (PDF)

AUTHOR INFORMATION

Corresponding Authors

*E-mail: rpr@miami.edu (R.P.).
*E-mail: psen@iitk.ac.in (P.S.).
*E-mail: murthy1@miami.edu (V.R.).

ORCID

Rajeev Prabhakar: 0000-0003-1137-1272
Pratik Sen: 0000-0002-8202-1854
Vaidhyanathan Ramamurthy: 0000-0002-3168-2185

Notes

The authors declare no competing financial interest.

ACKNOWLEDGMENTS

V.R. and R.P. thank the National Science Foundation (CHE-1807729 and CHE-1664926, respectively) for financial support. P.S. and A.D. thank Visvesvaraya PhD Program of Ministry of Electronics & Information Technology (MeitY), Government of India for providing young faculty research fellowship and graduate fellowship respectively.

REFERENCES

(1) Ramamurthy, V. *Photochemistry in Organized & Constrained Media*; VCH: New York, 1991.
(2) Ramamurthy, V.; Inoue, Y. *Supramolecular Photochemistry*; John Wiley: Hoboken, 2011.
(3) Brinker, U. H.; Mieusset, J.-L. *Molecular Encapsulation*; John Wiley & Sons: Chichester, 2010.
(4) Breslow, R. *Artificial Enzymes*; Wiley-VCH: Weinheim, 2005.
(5) Yoshizawa, M.; Fujita, M. Self-Assembled Coordination Cage as a Molecular Flask. *Pure Appl. Chem.* **2005**, *77*, 1107–1112.
(6) Ajami, D.; Rebek, J. More Chemistry in Small Spaces. *Acc. Chem. Res.* **2013**, *46*, 990–999.
(7) Murray, J.; Kim, K.; Ogoshi, T.; Yao, W.; Gibb, B. C. The aqueous supramolecular chemistry of cucurbit[n]urils, pillar[n]arenes and deep-cavity cavitands. *Chem. Soc. Rev.* **2017**, *46*, 2479–2496.
(8) Turro, N. J. Fun with Photons, Reactive Intermediates, and Friends. Skating on the Edge of the Paradigms of Physical Organic Chemistry, Organic Supramolecular Photochemistry, and Spin Chemistry. *J. Org. Chem.* **2011**, *76*, 9863.
(9) Ramamurthy, V. Organic Photochemistry in Organized Media. *Tetrahedron* **1986**, *42*, 5753–5839.
(10) Ramamurthy, V.; Sivaguru, J. Supramolecular Photochemistry as a Potential Synthetic Tool: Photocycloaddition. *Chem. Rev.* **2016**, *116*, 9914–9993.
(11) Ramamurthy, V.; Jockusch, S.; Porel, M. Supramolecular Photochemistry in Solution and on Surfaces: Encapsulation and Dynamics of Guest Molecules and Communication between Encapsulated and Free Molecules. *Langmuir* **2015**, *31*, 5554–5570.
(12) Ramamurthy, V. Photochemistry within a Water-Soluble Organic Capsule. *Acc. Chem. Res.* **2015**, *48*, 2904–2917.
(13) Gibb, C. L. D.; Gibb, B. C. Well-Defined, Organic Nanoenvironments in Water: The Hydrophobic Effect Drives a Capsular Assembly. *J. Am. Chem. Soc.* **2004**, *126*, 11408–11409.
(14) Jayaraj, N.; Zhao, Y.; Parthasarathy, A.; Porel, M.; Liu, R. S. H.; Ramamurthy, V. Nature of Supramolecular Complexes Controlled by the Structure of the Guest Molecules: Formation of Octa Acid Based Capsuleplex and Cavitandplex. *Langmuir* **2009**, *25*, 10575–10586.
(15) Porel, M.; Jayaraj, N.; Kaanumalle, L. S.; Maddipatla, M. V. S. N.; Parthasarathy, A.; Ramamurthy, V. Cavitand Octa Acid Forms a Nonpolar Capsuleplex Dependent on the Molecular Size and Hydrophobicity of the Guest. *Langmuir* **2009**, *25*, 3473–3481.

DOI: 10.1021/acs.jpca.9b04626
J. Phys. Chem. A 2019, 123, 5928–5936

(16) Kulasekharan, R.; Jayaraj, N.; Porel, M.; Choudhury, R.; Sundaresan, A. K.; Parthasarathy, A.; Ottaviani, M. F.; Jockusch, S.; Turro, N. J.; Ramamurthy, V. Guest Rotations within a Capsuleplex Probed by Nmr and Epr Techniques. *Langmuir* **2010**, *26*, 6943−6953.
(17) Jayaraj, N.; Jockusch, S.; Kaanumalle, L. S.; Turro, N. J.; Ramamurthy, V. Dynamics of capsuleplex formed between octaacid and organic guest molecules - Photophysical techniques reveal the opening and closing of capsuleplex. *Can. J. Chem.* **2011**, *89*, 203−213.
(18) Tang, H.; de Oliveira, C. S.; Sonntag, G.; Gibb, C. L. D.; Gibb, B. C.; Bohne, C. Dynamics of a Supramolecular Capsule Assembly with Pyrene. *J. Am. Chem. Soc.* **2012**, *134*, 5544−5547.
(19) Chuang, C.-H.; Porel, M.; Choudhury, R.; Burda, C.; Ramamurthy, V. Ultrafast Electron Transfer across a Nanocapsular Wall: Coumarins as Donors, Viologen as Acceptor, and Octa Acid Capsule as the Mediator. *J. Phys. Chem. B* **2018**, *122*, 328−337.
(20) Porel, M.; Chuang, C.-H.; Burda, C.; Ramamurthy, V. Ultrafast Photoinduced Electron Transfer between an Incarcerated Donor and a Free Acceptor in Aqueous Solution. *J. Am. Chem. Soc.* **2012**, *134*, 14718−14721.
(21) Raj, A. M.; Porel, M.; Mukherjee, P.; Ma, X.; Choudhury, R.; Galoppini, E.; Sen, P.; Ramamurthy, V. Ultrafast Electron Transfer from Upper Excited State of Encapsulated Azulenes to Acceptors across an Organic Molecular Wall. *J. Phys. Chem. C* **2017**, *121*, 20205−20216.
(22) Porel, M.; Jockusch, S.; Ottaviani, M. F.; Turro, N. J.; Ramamurthy, V. Interaction between Encapsulated Excited Organic Molecules and Free Nitroxides: Communication across a Molecular Wall. *Langmuir* **2011**, *27*, 10548−10555.
(23) Jockusch, S.; Porel, M.; Ramamurthy, V.; Turro, N. J. Cidep from a Polarized Ketone Triplet State Incarcerated within a Nanocapsule to a Nitroxide in the Bulk Aqueous Solution. *J. Phys. Chem. Lett.* **2011**, *2*, 2877−2880.
(24) Jockusch, S.; Zeika, O.; Jayaraj, N.; Ramamurthy, V.; Turro, N. J. Electron Spin Polarization Transfer from a Nitroxide Incarcerated within a Nanocapsule to a Nitroxide in the Bulk Aqueous Solution. *J. Phys. Chem. Lett.* **2010**, *1*, 2628−2632.
(25) Chen, J. Y.-C.; Jayaraj, N.; Jockusch, S.; Ottaviani, M. F.; Ramamurthy, V.; Turro, N. J. An EPR and NMR Study of Supramolecular Effects on Paramagnetic Interaction between a Nitroxide Incarcerated within a Nanocapsule with a Nitroxide in Bulk Aqueous Media. *J. Am. Chem. Soc.* **2008**, *130*, 7206−7207.
(26) Gupta, S.; Adhikari, A.; Mandal, A. K.; Bhattacharyya, K.; Ramamurthy, V. Ultrafast Singlet-Singlet Energy Transfer between an Acceptor Electrostatically Attached to the Walls of an Organic Capsule and the Enclosed Donor. *J. Phys. Chem. C* **2011**, *115*, 9593−9600.
(27) Samanta, S. R.; Parthasarathy, A.; Ramamurthy, V. Supramolecular Control During Triplet Sensitized Geometric Isomerization of Stilbenes Encapsulated in a Water Soluble Organic Capsule. *Photochem. Photobiol. Sci.* **2012**, *11*, 1652−1660.
(28) Jayaraj, N.; Jagadesan, P.; Samanta, S. R.; Da Silva, J. P.; Ramamurthy, V. Release of Guests from Encapsulated Masked Hydrophobic Precursors by a Phototrigger. *Org. Lett.* **2013**, *15*, 4374−4377.
(29) Jagadesan, P.; Da Silva, J. P.; Givens, R. S.; Ramamurthy, V. Photorelease of Incarcerated Guests in Aqueous Solution with Phenacyl Esters as the Trigger. *Org. Lett.* **2015**, *17*, 1276−1279.
(30) Kamatham, N.; Mendes, D. C.; Da Silva, J. P.; Givens, R. S.; Ramamurthy, V. Photorelease of Incarcerated Caged Acids from Hydrophobic Coumaryl Esters into Aqueous Solution. *Org. Lett.* **2016**, *18*, 5480−5483.
(31) Kamatham, N.; Da Silva, J. P.; Givens, R. S.; Ramamurthy, V. Melding Caged Compounds with Supramolecular Containers: Photogeneration and Miscreant Behavior of the Coumarylmethyl Carbocation. *Org. Lett.* **2017**, *19*, 3588−3591.
(32) Mohan Raj, A.; Raymo, F. M.; Ramamurthy, V. Reversible Disassembly-Assembly of Octa Acid-Guest Capsule in Water Triggered by a Photochromic Process. *Org. Lett.* **2016**, *18*, 1566−1569.
(33) Horng, M. L.; Gardecki, J. A.; Papazyan, A.; Maroncelli, M. Subpicosecond Measurements of Polar Solvation Dynamics: Coumarin 153 Revisited. *J. Phys. Chem.* **1995**, *99*, 17311−17337.
(34) Maroncelli, M.; Fleming, G. R. Comparison of time-resolved fluorescence Stokes shift measurements to a molecular theory of solvation dynamics. *J. Chem. Phys.* **1988**, *89*, 875−881.
(35) Maroncelli, M.; Fleming, G. R. Picosecond Solvation Dynamics of Coumarin 153: The Importance of Molecular Aspects of Solvation. *J. Chem. Phys.* **1987**, *86*, 6221−6239.
(36) Jarzeba, W.; Walker, G. C.; Johnson, A. E.; Kahlow, M. A.; Barbara, P. F. Femtosecond Microscopic Solvation Dynamics of Aqueous Solutions. *J. Chem. Phys.* **1988**, *92*, 7039−7041.
(37) Kahlow, M. A.; Jarzęba, W. o.; Kang, T. J.; Barbara, P. F. Femtosecond Resolved Solvation Dynamics in Polar Solvents. *J. Chem. Phys.* **1989**, *90*, 151−158.
(38) Jones, G.; Jackson, W. R.; Choi, C. Y.; Bergmark, W. R. Solvent Effects on Emission Yield and Lifetime for Coumarin Laser Dyes. Requirements for a Rotatory Decay Mechanism. *J. Phys. Chem. C* **1985**, *89*, 294−300.
(39) Nandi, N.; Bhattacharyya, K.; Bagchi, B. Dielectric Relaxation and Solvation Dynamics of Water in Complex Chemical and Biological Systems. *Chem. Rev.* **2000**, *100*, 2013−2046.
(40) Bhattacharyya, K. Solvation Dynamics and Proton Transfer in Supramolecular Assemblies. *Acc. Chem. Res.* **2003**, *36*, 95−101.
(41) Datta, A.; Pal, S. K.; Mandal, D.; Bhattacharyya, K. Solvation Dynamics of Coumarin 480 in Vesicles. *J. Phys. Chem. B* **1998**, *102*, 6114−6117.
(42) Sarkar, N.; Das, K.; Datta, A.; Das, S.; Bhattacharyya, K. Solvation Dynamics of Coumarin 480 in Reverse Micelles. Slow Relaxation of Water Molecules. *J. Phys. Chem.* **1996**, *100*, 10523−10527.
(43) Sarkar, N.; Datta, A.; Das, S.; Bhattacharyya, K. Solvation Dynamics of Coumarin 480 in Micelle. *J. Phys. Chem.* **1996**, *100*, 15483−15486.
(44) Das, K.; Sarkar, N.; Das, S.; Datta, A.; Bhattacharyya, K. Solvation Dynamics in a Solid Host. Coumarin 480 in Zeolite 13x. *Chem. Phys. Lett.* **1996**, *249*, 323−328.
(45) Pal, S. K.; Sukul, D.; Mandal, D.; Sen, S.; Bhattacharyya, K. Solvation Dynamics of Coumarin 480 in Sol−Gel Matrix. *J. Phys. Chem. B* **2000**, *104*, 2613−2616.
(46) Sen, P.; Mukherjee, S.; Halder, A.; Bhattacharyya, K. Temperature dependence of solvation dynamics in a micelle. 4-Aminophthalimide in Triton X-100. *Chem. Phys. Lett.* **2004**, *385*, 357−361.
(47) Sen, P.; Mukherjee, S.; Patra, A.; Bhattacharyya, K. Solvation Dynamics of DCM in a DPPC Vesicle Entrapped in a Sodium Silicate Derived Sol−Gel Matrix. *J. Phys. Chem. B* **2005**, *109*, 3319−3323.
(48) Sen, P.; Roy, D.; Mondal, S. K.; Sahu, K.; Ghosh, S.; Bhattacharyya, K. Fluorescence Anisotropy Decay and Solvation Dynamics in a Nanocavity: Coumarin 153 in Methyl β-Cyclodextrins. *J. Phys. Chem. A* **2005**, *109*, 9716−9722.
(49) Mukherjee, P.; Das, A.; Sen, P. Solvation Dynamics in SDS Micelle Revisited with Femtosecond Time Resolution to Reveal the Probe and Concentration Dependence. *Chem. Phys.* **2018**, *513*, 141−148.
(50) Choudhury, R.; Barman, A.; Prabhakar, R.; Ramamurthy, V. Hydrocarbons Depending on the Chain Length and Head Group Adopt Different Conformations within a Water-Soluble Nanocapsule: 1H NMR and Molecular Dynamics Studies. *J. Phys. Chem. B* **2013**, *117*, 398−407.
(51) Frisch, M. J.; Trucks, G. W.; Schlegel, H. B.; Scuseria, G. E.; Robb, M. A.; Cheeseman, J. R.; Scalmani, G.; Barone, V.; Mennucci, B.; Petersson, G. A. *Gaussian 09*, Revision E.01; Gaussian, Inc., Wallingford CT, 2009.
(52) Becke, A. D. Density-functional thermochemistry. III. The role of exact exchange. *J. Chem. Phys.* **1993**, *98*, 5648−5652.
(53) Francl, M. M.; Pietro, W. J.; Hehre, W. J.; Binkley, J. S.; Gordon, M. S.; DeFrees, D. J.; Pople, J. A. Self-consistent molecular

DOI: 10.1021/acs.jpca.9b04626
J. Phys. Chem. A 2019, 123, 5928−5936

orbital methods. XXIII. A polarization-type basis set for second-row elements. *J. Chem. Phys.* **1982**, *77*, 3654−3665.
(54) Trott, O.; Olson, A. J. Autodock Vina: Improving the Speed and Accuracy of Docking with a New Scoring Function, Efficient Optimization, and Multithreading. *J. Comput. Chem.* **2010**, *31*, 455−461.
(55) Pronk, S.; Páll, S.; Schulz, R.; Larsson, P.; Bjelkmar, P.; Apostolov, R.; Shirts, M. R.; Smith, J. C.; Kasson, P. M.; Van Der Spoel, D.; Hess, B.; Lindahl, E. Gromacs 4.5: A High-Throughput and Highly Parallel Open Source Molecular Simulation Toolkit. *Bioinformatics* **2013**, *29*, 845−854.
(56) Case, D. A.; Cheatham, T. E., III; Darden, T.; Gohlke, H.; Luo, R.; Merz, K. M., Jr.; Onufriev, A.; Simmerling, C.; Wang, B.; Woods, R. J. The Amber Biomolecular Simulation Programs. *J. Comput. Chem.* **2005**, *26*, 1668−1688.
(57) Wang, J.; Wold, R. M.; Caldwell, J. W.; Case, D. A. Development and Testing of a General AMBER Force Field. *J. Comp. Chem.* **2004**, *25*, 1157−1174.
(58) Price, D. J.; Brooks, C. L., III A Modified Tip3p Water Potential for Simulation with Ewald Summation. *J. Chem. Phys.* **2004**, *121*, 10096−10103.
(59) Darden, T.; York, D.; Pedersen, L. Particle mesh Ewald: An N·log(N) method for Ewald sums in large systems. *J. Chem. Phys.* **1993**, *98*, 10089−10092.
(60) Miyamoto, S.; Kollman, P. A. Settle: An Analytical Version of the Shake and Rattle Algorithm for Rigid Water Models. *J. Comput. Chem.* **1992**, *13*, 952−962.
(61) Hess, B.; Bekker, H.; Berendsen, H. J. C.; Fraaije, J. G. E. M. Lincs: A Linear Constraint Solver for Molecular Simulations. *J. Comput. Chem.* **1997**, *18*, 1463−1472.
(62) Krieger, E.; Vriend, G. YASARA View-molecular graphics for all devices-from smartphones to workstations. *Bioinformatics* **2014**, *30*, 2981−2982.
(63) Pettersen, E. F.; Goddard, T. D.; Huang, C. C.; Couch, G. S.; Greenblatt, D. M.; Meng, E. C.; Ferrin, T. E. UCSF Chimera?A visualization system for exploratory research and analysis. *J. Comput. Chem.* **2004**, *25*, 1605−1612.
(64) Humphrey, W.; Dalke, A.; Schulten, K. Vmd: Visual Molecular Dynamics. *J. Mol. Graphics* **1996**, *14*, 33−38.

DOI: 10.1021/acs.jpca.9b04626
J. Phys. Chem. A 2019, 123, 5928−5936